

# Synthesis and Thin Film Characterization of Poly(styrene-*block*-methyl methacrylate) Containing an Anthracene Dimer Photocleavable Junction Point

James T. Goldbach, Thomas P. Russell,\* and Jacques Penelle\*

Department of Polymer Science and Engineering, University of Massachusetts at Amherst, Amherst, Massachusetts 01003-4530

Received November 6, 2001; Revised Manuscript Received March 5, 2002

**ABSTRACT:** Telechelic high molecular weight polystyrene (PS-A) and poly(methyl methacrylate) (PMMA-A) containing anthracene end groups undergo end-coupling reaction in THF solution to form  $[4 + 4]$  anthracene photodimers upon exposure to UV irradiation at wavelengths greater than 300 nm. A mixture of products is obtained that include the coupled polystyrene homopolymer, P(S-AA-S), coupled PMMA homopolymer, P(MMA-AA-MMA), and the desired diblock copolymer, P(S-AA-MMA). The polymer concentration and molecular weights have a direct influence on the photoreaction kinetics but do not affect the molar ratio of the three polymeric products. P(S-AA-MMA), purified by extraction of the homopolymers with selective solvents, exhibits thermal cleavage of the junction points and reversion back to homopolymers at temperatures at or above 135 °C. AFM images of thin films of P(S-AA-MMA) spin-coated onto passivated silicon substrates show a microphase-separated cylindrical microdomain morphology with the cylinders oriented normal to the surface.

## Introduction

It has been demonstrated that structured membranes with a regular array of nanopores spanning the entire film thickness can be easily fabricated from thin-film templates made of poly(styrene-*block*-methyl methacrylate) (P(S-*b*-MMA)) copolymers.<sup>1–5</sup> The final porous structure is generated from the template by selective degradation of the poly(methyl methacrylate) (PMMA) blocks that constitute the cylinders in the microphase-separated morphology obtained when the relative volume fraction of each block in the P(S-*b*-MMA) copolymer is maintained at a ratio of about 70:30. Orientation of the cylinders normal to the surface in the thin films can be realized prior to the final degradation step by application of an external electric field<sup>6–9</sup> or control of the interfacial interactions.<sup>10–13</sup>

In the above example, the final porous structure is obtained from the oriented polymeric template by UV photoirradiation of the thin polymeric film.<sup>1</sup> This harsh, yet effective, treatment induces the almost simultaneous cross-linking of the polystyrene (PS) continuous phase and the degradation of the PMMA cylinders to smaller molecules that can be removed by subsequent solvent treatment. Although this approach is easy to implement, the poor chemical selectivity of the UV treatment leads to membranes where the nature of functional groups available at the surface of the film and inside the pores is not well-defined. This strategy is very efficient for numerous applications (for example, the resulting nanoporous membranes have been used as templates for the electrochemical fabrication of arrays of nanowires),<sup>2,14,15</sup> but it is also fundamentally incompatible with the requirements needed for other applications, such as the fabrication of reactive biomembranes where the covalent attachment of enzymes inside the nanopores specifically requires a better controlled chemistry and the possibility to selectively decorate the walls of the nanopores, with little or no reactive functionalities present on top of the film.

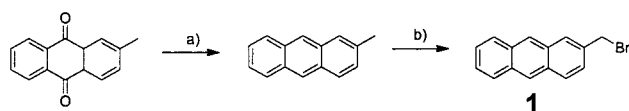
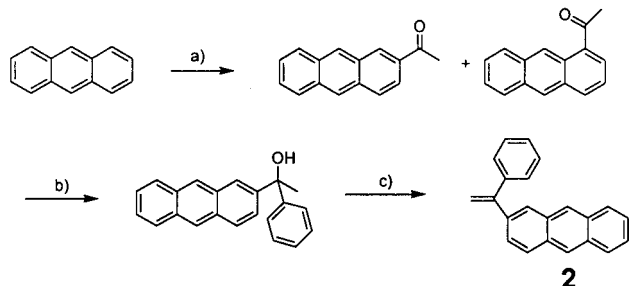
A possible way to solve this problem is to place a UV-photocleavable unit at the junction point between the

two blocks. During the photoirradiation step, a well-defined functionality can then be generated selectively on the pore walls. In this contribution, results obtained using the  $[4 + 4]$  photodimer of anthracene as the photocleavable junction point in a 72K (70:30 v/v) P(S-*b*-MMA) diblock copolymer are described. This contribution is the first of a series dealing with the synthesis, morphology, physics, and use of diblock copolymers containing photocleavable units at the junction point between the two blocks.

On the basis of its known chemistry,<sup>16</sup> the  $[4 + 4]$  photodimer of anthracene should provide lability at a narrow range of wavelengths of UV radiation, stability at elevated temperatures, quantitative cleavage upon irradiation, production of specific functional groups left behind after cleavage, and absorption at a wavelength that will not degrade either polymer block. Most importantly, anthracene photodimers are cleaved to two anthracene units by irradiation at 280 nm and are stable above the glass transition temperature of PS and PMMA, which should permit thermal annealing of thin films of this copolymer.<sup>17,18</sup> Availability of these diblock copolymers also opens the possibility of further study on the physics of diblock copolymer microphase separation, fluctuations at interfaces of highly thermodynamically frustrated systems, investigation of the  $T_g$  of nanometer-scale confined homopolymer domains, and a route to study the kinetics of phase separation in homopolymer mixtures. These issues are currently under investigation in our groups as well as in collaborations and will be described in future publications.

## Experimental Section

**General Procedures and Materials.** All polymerizations and water/air-sensitive manipulations were carried out using standard Schlenk techniques<sup>19</sup> under a dry nitrogen atmosphere. Tetrahydrofuran (THF) and benzene were distilled under nitrogen from purple sodium/benzophenone ketyl. Styrene and methyl methacrylate (MMA) were purchased from Aldrich and vacuum-distilled from calcium hydride just before use. Reagents for the synthesis of end-capping agents were

**Scheme 1. Synthesis of 1:** (a)  $\text{NH}_3(\text{aq})$ , Zn, Reflux 7 h; (b)  $\text{CCl}_4$ , NBS, Reflux**Scheme 2. Synthesis of 2:** (a) Nitrobenzene,  $\text{AlCl}_3$ , 15 °C, 12 h; (b) THF,  $\text{PhMgBr}$ , Reflux; (c) Acetic Acid, 100 °C, 1 h

purchased from Aldrich and used as received. End-capping agents **1** and **2** (Schemes 1 and 2, respectively) were synthesized as described previously.<sup>20–23</sup>

**Instrumentation.** Gel permeation chromatograms (GPC) were obtained on an in-house built GPC system using PL Caliber data collection software, three-column set (Polymer Labs, Inc.;  $300 \times 7.5$  mm,  $5 \mu\text{m}$ ,  $10^{-5}$ ,  $10^{-4}$ , and  $10^{-3}$  Å), with variable UV (IBM model, LC 9563) and RI (Waters 403) detectors. The system was calibrated with respect to polystyrene and poly(methyl methacrylate) standards (Polymer Labs, Inc.).  $^1\text{H}$  and  $^{13}\text{C}$  NMR spectra were obtained on a Bruker DPX-300 spectrometer using  $\text{CDCl}_3$  as solvent. AFM images were obtained using a Digital Instruments Dimension 3000 atomic force microscope in tapping mode with etched silicon tips (Nanoprobe). The spring constant of the tips was  $40\text{--}66 \text{ N m}^{-1}$  as specified by the manufacturer. Film thicknesses were measured at a 70° incidence angle by ellipsometry using a Rudolph Research AutoEl-II ellipsometer equipped with a helium–neon laser.

**Polystyrene End-Functionalized with 2-(Bromomethyl)anthracene (1) (PS-A).** A heat-dried, nitrogen-purged 100 mL flask was charged with 50 mL of dry benzene. 3.0 mL of freshly distilled styrene was added via syringe. 0.075 mL of  $1.3 \text{ mol L}^{-1}$  sBuLi was added with rapid stirring, producing an orange-red solution. This solution was kept at room temperature for 2 h with rapid stirring. In another heat-dried, nitrogen-purged 100 mL flask were added 10 mL of dry benzene and 0.1220 g of vacuum-dried **1**. The polystyryllithium solution was then added to the solution of **1** via cannula with rapid stirring. A very rapid color change from red-orange to purple to faint yellow was observed, and this solution was stirred for 5 min at room temperature. The polymer was then precipitated in methanol, dissolved, and reprecipitated twice to remove excess **1**. GPC (PS standard)  $\bar{M}_n = 30\text{K}$ ;  $\bar{M}_w/\bar{M}_n = 1.05$ .

**Polystyrene End-Functionalized with 1-Phenyl-1-(2-anthryl)ethylene (2) (PS-A).** A heat-dried, nitrogen-purged, 250 mL flask was charged with 200 mL of dry THF and cooled to  $-78^\circ\text{C}$  under nitrogen. 0.140 mL of  $1.0 \text{ mol L}^{-1}$  sBuLi was added via a syringe. 10.0 mL of freshly distilled styrene was then added via a syringe with rapid stirring, giving an orange solution. This solution was stirred at  $-78^\circ\text{C}$  for 5 min. Concurrently, a second 250 mL heat-dried, nitrogen-purged flask was charged with 5.0 mL of dry THF and 0.0770 g (1.5 equiv of **2** to sBuLi) of vacuum-dried **2** and cooled to  $-78^\circ\text{C}$ . A few drops of sBuLi were added to this solution until a slight purple color persisted. The living polystyryllithium solution was then added to the solution of **2** via 16 G cannula, affording a deep purple solution. This solution was stirred at  $-78^\circ\text{C}$  for 5 min. 1.0 mL of degassed methanol was then added via a syringe. This faintly yellow polymer solution was then precipitated in 1.0 L of methanol, filtered, and dried in vacuo. It

was then redissolved in 200 mL of toluene and forced with air pressure through a column of alumina with one column volume of toluene eluent. This purified polymer was again precipitated in 1.0 L of methanol, filtered, and dried in vacuo. GPC (PS standards):  $\bar{M}_n = 51.0\text{K}$ ;  $\bar{M}_w/\bar{M}_n = 1.04$ .

**Anthracene End-Functionalized Poly(methyl methacrylate) (PMMA-A).** To a heat-dried, nitrogen-purged 250 mL flask, 0.1250 g (0.446 mmol) of dry **2** was added and dried under vacuum for 12 h at  $50^\circ\text{C}$ . Upon cooling under nitrogen, 175 mL of THF was added via cannula and cooled to  $-78^\circ\text{C}$ . 0.350 mL of  $1.3 \text{ mol L}^{-1}$  sBuLi was added via a syringe, giving rise to a deep purple color. 10.0 mL of freshly distilled MMA was added slowly via a syringe under rapid stirring. The slightly yellow solution was stirred for an additional 10 min at  $-78^\circ\text{C}$ , and then 1.0 mL of degassed methanol was added via a syringe. The polymer was precipitated in 1.0 L of hexanes, filtered, and dried in vacuo. GPC (PMMA standards):  $\bar{M}_n = 21.0\text{K}$ ;  $\bar{M}_w/\bar{M}_n = 1.10$ .

**PS-A and PMMA-A UV Photocoupling.** 2.0 g of PS-A (51K) and 1.0 g of PMMA-A (21K) were added to a dry 100 mL round-bottom flask (borosilicate glass) and dried under vacuum for 12 h. The flask was evacuated and back-filled with nitrogen three times, and then 30.0 mL of dry, degassed THF was added via cannula. The flask was sealed and exposed to 300–360 nm UV radiation from a 100 W spot source through its fiber-optic light guide (Dymax, UV Products Co.) for 150 h. The flask was opened, and the polymer was precipitated in 300 mL of hexanes, filtered, and dried in vacuo. Using a double-thickness extraction thimble, the polymer mixture was continuously extracted with cyclohexane in a Soxhlet apparatus for 48 h. The remaining polymer was reprecipitated in a mixture of isomeric hexanes, dried, and stirred consecutively for 12 h each with methanol, acetic acid, and then continuously extracted with acetonitrile again in a Soxhlet apparatus. The purified diblock copolymer was filtered and dried in vacuo. GPC (PS standards):  $\bar{M}_n = 72.0\text{K}$ ;  $\bar{M}_w/\bar{M}_n = 1.05$ .

**Silicon Substrate and Thin Film Preparation.** 100 mm diameter silicon (100) wafers (International Wafer Service) were scored and fractured into  $2 \text{ cm}^2$  squares. Passivated surfaces were prepared by immersing each wafer in 6% (w/v) aqueous HF solution for 120 s, followed by rinsing with deionized water and drying with nitrogen.  $\text{SiO}_2$  surfaces were prepared by washing the native  $\text{SiO}_2$  surface with filtered toluene. Films were spin-coated from 1% solutions in toluene and annealed under vacuum.

## Results and Discussion

The general design for the synthesis of the P(S-*b*-MMA) diblock copolymer discussed in this paper is based on the statistical coupling of PS and PMMA macromolecules containing a photoreactive anthracene end group. The synthetic strategy is summarized in Scheme 1. Based on the final cylindrical morphology targeted in this study, molecular weights of  $51.0 \times 10^3$  and  $21.0 \times 10^3$  were selected for the PS and PMMA precursors, respectively.

**Synthesis of Anthracene End-Functionalized PS (PS-A).** Two procedures were considered for the efficient end-functionalization of polystyryllithium. The first involves the use of 2-(bromomethyl)anthracene, **1**, which was synthesized according to the procedure outlined in Scheme 2. Its use for the end-capping of living polystyryllithium in benzene afforded anthracene end-functionalized PS of the expected molecular weight as well as a considerable amount ( $>20\%$  of total) of a product with exactly double the expected molecular weight (Figure 1a). This impurity, which also had anthracene incorporated into the chain, was observed by GPC with the UV detector at 330 nm (Figure 1b). At this wavelength, only the anthracene units absorb radiation, while the phenyl rings on the PS are essentially invisible.

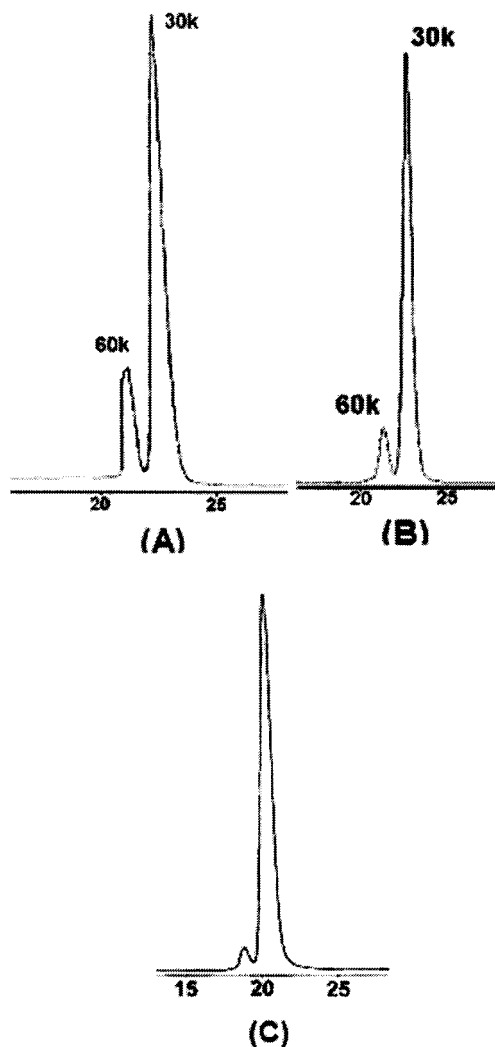


**Figure 1.** GPC chromatograms of PS after end-functionalization with anthracene-containing end-capping agents: (A) PS end-capped with **1**, UV detector at 254 nm; (B) PS end-capped with **1**, UV detector at 330 nm; (C) PS end-capped with **2**, UV detector at 254 nm.

Coursan et al.<sup>24</sup> previously reported experiments using 9-(chloromethyl)anthracene in a fashion similar to end-functionalize polystyryllithium. Along with the presence of unfunctionalized chains, they also observed a polystyryl polymer of the double molecular weight and proposed a mechanism of single electron transfer from polystyryllithium to 9-(chloromethyl)anthracene, followed by a subsequent dimerization of the obtained polystyrene free radicals. It was not reported whether the polystyrene impurity contains any anthryl unit, as in our case. In the absence of this crucial piece of evidence, the mechanism proposed by these authors, which does not provide for the existence of an anthracene unit in the polystyrene "dimer", cannot be ruled out. One alternate mechanism for the side reaction, which would both rationalize the formation of a "dimeric" polystyrene impurity *and* the presence of an anthracene unit (P(S-A-S)), can be tentatively based on a competing side reaction where a polystyryllithium attacks the anthracene ring itself on an already functionalized polystyrene, followed by a rearomatization (Scheme 3).

To test this hypothesis, a low molecular weight polystyryllithium synthesized in benzene at room temperature under the same conditions as those described above was added to a benzene solution of anthracene

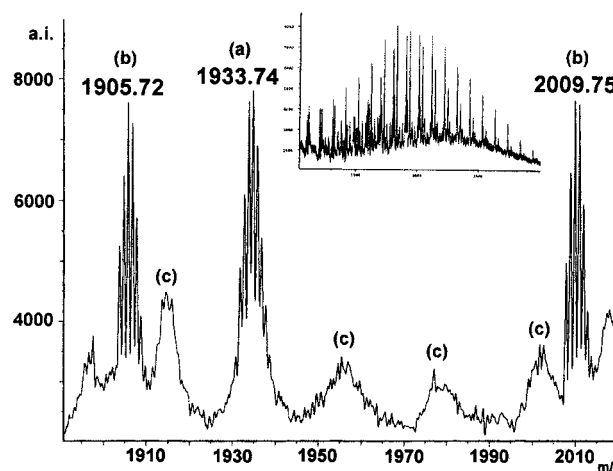
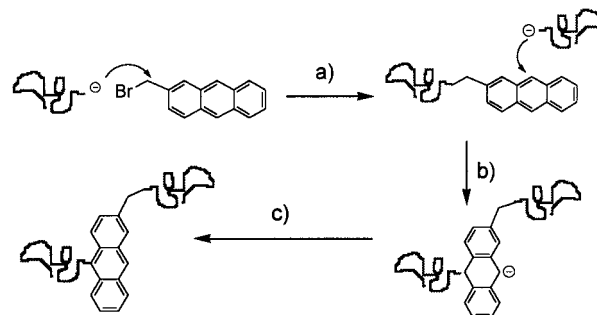


**Figure 2.** MALDI-ToF spectrum of ~2K polystyryllithium reacted with anthracene in benzene at room temperature. Two major distributions correspond to PS with hydrogen end group (1933.74 Da) and PS with anthracene end group (1905.72 Da).

**Scheme 3. Proposed Mechanism for PS-Li Direct Attack on Anthracene as a Side Reaction to Form "Dimeric" PS Containing Anthracene Middle Group:**  
(a)  $S_N2$  Substitution of Bromine by Polystyryllithium;  
(b) Nucleophilic Attack on Anthracene Ring by Second Polystyryllithium;  
(c) Rearomatization Back to Anthracene



(same amount and concentration as the solution of **1** discussed above). Upon addition, the orange-red color of the polystyryllithium solution rapidly changed to a persistent red-purple color, suggesting addition to the polystyryllithium carbanion. MALDI-ToF analysis of the polymer product obtained after addition of methanol and drying provided a spectrum with peaks consistent with polystyrene chains containing (a) hydrogen end groups (from the reaction of polystyryllithium with methanol), (b) anthracene units, and (c) end groups of unknown structure. An expanded view of the entire spectrum is provided in Figure 2, which indicates that the two most intense distributions (PS-H and PS-A) are in an almost one-to-one ratio (the PS-H  $Ag^+$  adduct signal is contaminated by another smaller signal at slightly lower mass) and account for most of the entire signal.

The presence of a significant amount of a polystyryl "dimeric" impurity containing an anthracene unit in the middle made the use of **1** as an end-capping agent an unsuitable method for anthracene end-functionalization of PS. As will be seen later, if this polymer mixture were to be used in the subsequent UV end-coupling reactions, a significant amount of triblock star copolymer from the reaction of P(S-A-S) with PMMA-A would be formed. To alleviate this problem, an attempt was made to use 1-phenyl-1-(2-anthryl)ethylene (**2**) as the end-capping agent. Winnik et al.<sup>25-28</sup> have already shown that moieties such as **2** are very useful for chromophoric



labeling of the junction point in P(S-*b*-MMA) diblock copolymers. Their previous work indicates that polystyryllithium rapidly adds to **2** and that the anion formed efficiently initiates MMA polymerization. The addition of polystyryllithium to the double bond in **2** can be expected to be more rapid than the substitution of bromine on **1**. The ceiling temperature for polymerization of **2** is very low, so there is no oligomerization and only one anthryl unit is incorporated at the end of the polystyrene chain. Also, the anion formed is more sterically hindered than the carbanion end of polystyryllithium and therefore less able to participate in the side reaction of adding on to an anthracene ring. The end-capping agent was synthesized in three steps summarized in Scheme 2.

Using previously described conditions for the synthesis of a  $\bar{M}_n = 30\text{K}$  polystyryllithium and **2** as the end-capping agent, the occurrence of the decoupling side reaction so that the amount of decoupled product was less than 5% of the total (Figure 1c). Characterization by GPC indicated that the expected molecular weight was obtained, and the molecular weight distribution is narrow ( $\bar{M}_w/\bar{M}_n = 1.04$ ). Characterization of the final PS-A polymer by  $^1\text{H}$  NMR also agrees with the expected structure.

**Synthesis of Anthracene End-Functionalized PMMA (PMMA-A).** As discussed above, Winnik et al. have shown that the anionic macro adduct of **2** is an efficient initiator for the initiation of MMA polymerization. They have proficiently used **2** and other diphenylethylene-like moieties to label the junction points of diblock copolymers. With their results in mind, addition of *sec*-butyllithium on **2** and use of this adduct as initiator for anionic polymerization of MMA in THF at  $-78^\circ\text{C}$  was a logical approach to obtain a high degree of functionalization for the PMMA chains. Experimentally, MMA was added at  $-78^\circ\text{C}$  to a rapidly stirred THF solution of an anionic adduct of **2**, generated by adding *sec*-BuLi to **2**. The deep purple color of the initiator solution immediately changed to a very pale yellow upon the addition of MMA, indicating rapid initiation by the anthryl anionic initiator. GPC results obtained after the addition of methanol, drying, and precipitation in hexanes showed a polymer of the expected molecular weight  $\bar{M}_n = 21\text{K}$  and low-polydispersity monomodal distribution ( $\bar{M}_w/\bar{M}_n \sim 1.1$ ) had been obtained. MALDI-ToF analysis of a low molecular weight sample ( $\bar{M}_n = 2.0\text{K}$ ) reveals two distributions corresponding to the sodium and potassium adducts of anthracene-functionalized PMMA (Figure 3a, peaks 1 and 2, respectively) and a very weak signal from an unidentified impurity (Figure 3a, peak 3). The  $^1\text{H}$  NMR of the polymer is in agreement with the proposed structure.

**Synthesis of a Photocleavable Diblock Copolymer (PS-AA-PMMA) via UV Coupling of PS-A and PMMA-A.** Bartz et al. and Coursan et al. independently showed that low molecular weight anthracene end-functionalized polystyrene and poly(methyl methacrylate) ( $\bar{M}_n < 10.0\text{K}$ ) can be photodimerized under UV irradiation at 366 nm and quantitatively decoupled by irradiation at 280 nm with no cross-linking or degradation of the polymers.<sup>24,29</sup> To the best of our knowledge, similar work has not been performed with higher molecular weight polymers or on mixtures of dissimilar anthracene end-functionalized polymers to form diblock copolymers.

PMMA-A ( $\bar{M}_n = 21\text{K}$ ) and the PS-A ( $\bar{M}_n = 51\text{K}$ ) synthesized by end-capping with **2** were mixed in a 1:1

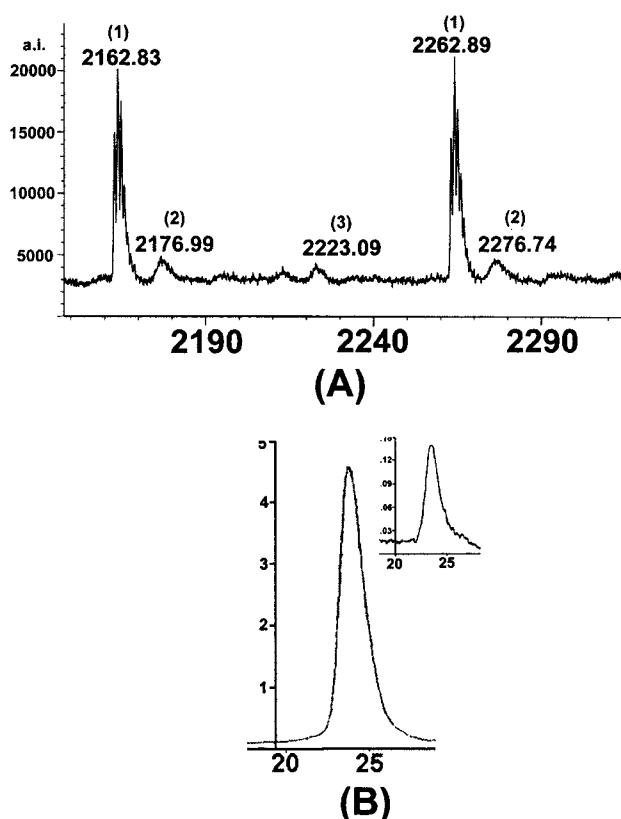


**Figure 3.** GPC and MALDI-ToF characterization of PMMA-A: (A) GPC with RI detector (inset: GPC with UV 330 nm detector); (B) expanded MALDI-ToF spectrum of  $\bar{M}_n = 2.0\text{K}$  PMMA initiated with **2**.

molar ratio and dissolved in degassed, dry THF under an atmosphere of dry nitrogen. This solution was irradiated with a high-intensity, 100 W UV spot source providing localized UV radiation at wavelengths above 300 nm, favoring the forward and coupling reaction. This type of UV source supplies a higher flux of photons per unit area than the standard UV lamp typically used in preparative photochemistry. A high flux is necessary because of the low quantum yield of the reaction. (In order for the UV photocycloaddition to occur, two chain ends to come in close proximity with one unit in its photoexcited state.) The photoexcited state only persists for a few nanoseconds, so it becomes crucial to provide as much UV radiation as possible to increase the relative concentration of excited anthryl end groups.

Under irradiation, the UV coupling reaction (Scheme 4) proceeded slowly, as expected, mainly due to relatively low concentration of anthryl chain ends. After 150 h of irradiation, the coupling products as well as unreacted homopolymers were observed by GPC (Figure 4a). The PS-A and P(S-AA-S) homopolymers were then removed from the mixture by extraction in a Soxhlet apparatus with cyclohexane as solvent (Figure 4b). To retain the diblock copolymer, it was important to use a double-thickness extraction thimble to prevent the diblock from being removed with the PS homopolymer. The remaining diblock copolymer, along with the PMMA homopolymer, was stirred in acetic acid for 24 h to selectively remove the PMMA homopolymer. This solution was filtered, and the remaining polymer was extracted for 48 h with acetonitrile to remove any residual PMMA homopolymer (24K and 48K). The GPC of the final, purified diblock copolymer showed no remaining PS or PMMA homopolymer, although a small

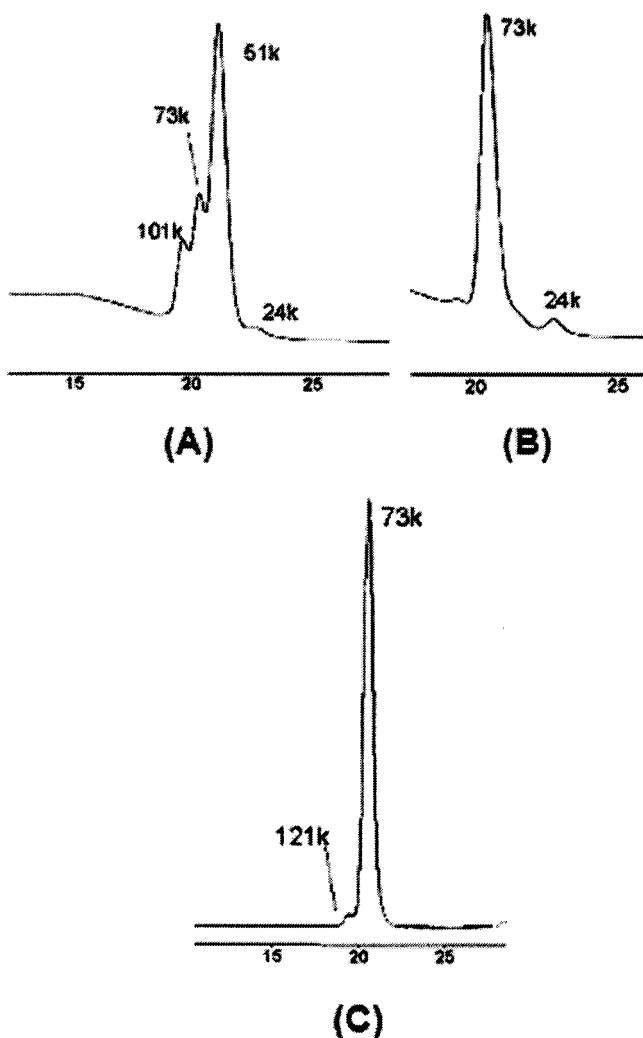
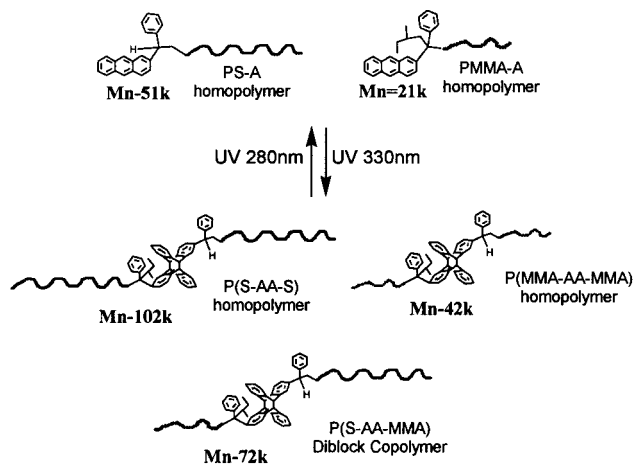


**Figure 4.** GPC traces of crude mixture after UV irradiation (A), mixture after cyclohexane extraction (B), and purified photocleavable diblock copolymer (C).

**Scheme 4. UV Coupling of Anthracene End-Functionalized PS and PMMA**



shoulder at  $\bar{M}_n = 121K$  that can possibly be explained by the formation of a P(S-A-MMA-A-S) triblock star copolymer (Figure 4c). As mentioned already, a small amount ( $\sim 5\%$ ) of polystyrene "dimeric" impurity contaminates the end-capped polystyrene reagent. This P(S-A-S) is theoretically able to photocouple with PMMA-A, forming a three-armed star copolymer with an

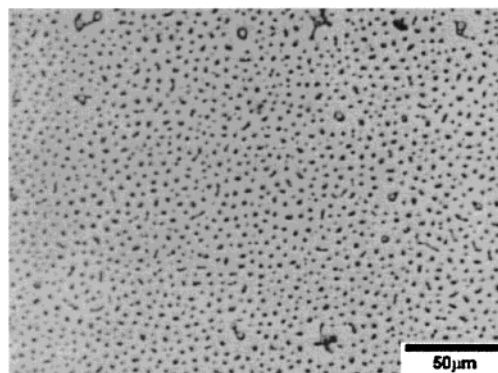


**Figure 5.** Optical micrograph of 30 nm thick film of P(S-AA-MMA) on passivated silicon, annealed at 190 °C for 2 h.

anthracene dimer at the core. This star, having one PMMA arm, cannot be extracted with cyclohexane, and having a large fraction of PS, was not washed out in the PMMA homopolymer extraction. The sample used for the subsequent thin film experiments contains this small amount of triblock.

**Temperature Stability of the Anthracene Dimer Junction Point in P(S-AA-MMA).** Many low-molecular-weight, [4 + 4] photodimers of substituted anthracene exhibit a melting point around 200 °C, where, upon melting, the photodimer reverts back to its two parent anthracenes. On the basis of these results, it can be expected that the P(S-AA-MMA) diblock copolymer will be stable at temperatures well above the glass transition temperature of either of the two blocks ( $\sim 100$  °C for a 51K PS and  $\sim 80$  °C for a 21K PMMA).<sup>30</sup> However, annealing thin films of P(S-AA-MMA) at 190 °C resulted in rapid cleavage of the junction point and phase separation of the homopolymers, as shown in the optical micrograph in Figure 5. Decreasing the annealing temperature to 170 °C resulted in slower cleavage of the junction point, yet phase separation was again observed within 6 h. Further decrease of the annealing temperature to 135 °C greatly slowed the degradation of the diblock copolymer, allowing microphase separation to occur. The mobility of the copolymer was also sufficiently high to allow the microdomains of the copolymer to assume a specific orientation. While GPC analysis of a P(S-AA-MMA) sample annealed at 135 °C for 48 h revealed that  $\sim 30\%$  scission had occurred. Sufficient diblock copolymer remained, however, to retain the microphase-separated structure.

**Thin Film Experiments Using the 72K P(S-AA-MMA) (70:30 v/v) Photocleavable Diblock Copolymer.** 30 nm thick films of the P(S-AA-MMA) diblock copolymer were spin-coated from toluene solutions onto passivated silicon substrates. As shown before, the interfacial interactions of PS and PMMA with passivated silicon are balanced, enabling an orientation of the copolymer microdomains normal to the surface.<sup>1</sup> Films were annealed under vacuum at 190 °C for 2 h, 170 °C for 6 h, or 135 °C for 48 h. AFM was used to examine the morphology in thin films. The self-assembly of the block copolymer into ordered microdomains was observed only for the sample annealed at 135 °C sample. PMMA cylinders with an average period of  $\sim 30$  nm are visible in a matrix of PS (Figure 6). The period and size of the microdomains are consistent with data for thin films of nonphotocleavable, anionically synthesized P(S-*b*-MMA).<sup>1</sup> Reduced mobility at 135 °C precluded attaining the equilibrium morphology where all of the micro-

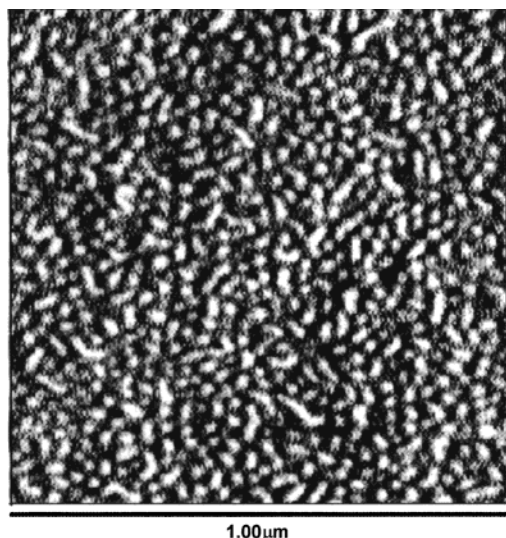


**Figure 6.** AFM phase image of a 30 nm thick film of P(S-AA-MMA) on passivated silicon, annealed at 135 °C for 48 h.

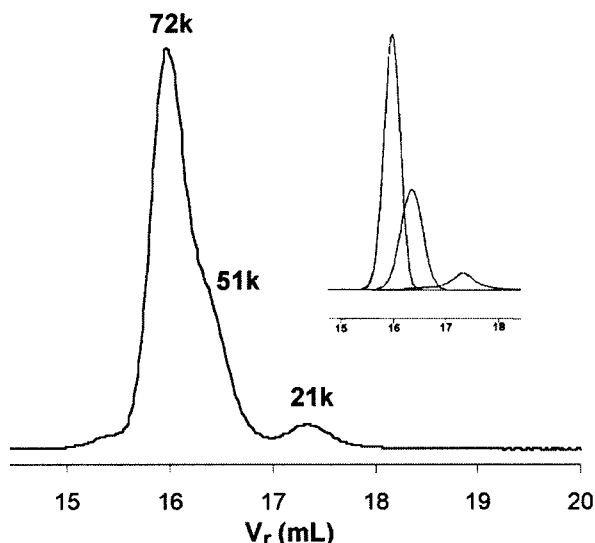


**Figure 7.** GPC chromatogram of P(S-AA-MMA) after heating at 135 °C for 48 h.

domains would be oriented normal to the surface. One approach to circumvent thermal degradation while enhancing dynamics would be to depress the glass transition temperature by the use of a plasticizer such as supercritical carbon dioxide. Investigations are in progress to examine this route.

## Conclusions

Anthracene end-functionalized PS and PMMA with narrow polydispersity and nearly monomodal distribution were synthesized using **2** as both an end-capping agent as well as an initiator for the anionic polymerization of styrene and methyl methacrylate, respectively. These anthracene end-functionalized polymers were UV-photocoupled in solution to form diblock copolymers with an anthracene [4 + 4] photodimer at the junction point between the blocks. Homopolymer byproducts were removed with selective solvents. The bisanthracene junction point was shown to be sensitive to temperatures at or above 135 °C, resulting in the cleavage of the diblock copolymer into homopolymers. Atomic force micrographs of thin films on passivated silicon surfaces showed microdomains of PMMA in a PS

matrix oriented normal to the surface. The thermal stability of the diblock copolymer prevented the use of thermal annealing alone to reach the full equilibrium morphology. Investigation of coupling kinetics, the UV cleavage reaction, and further studies on annealing conditions are currently underway.

**Acknowledgment.** Financial support by NSF Grant CTS-9871782, the NSF Partnership in Nanotechnology (DMR-9809365), and the University of Massachusetts Materials Research Science and Engineering Center (UMass-MRSEC) (DMR-8909365) shared facilities is gratefully acknowledged.

## References and Notes

- (1) Xu, T.; DeRouchey, J.; Seney, C.; Levesque, C.; Martin, P.; Stafford, C. M.; Russell, T. P. *Polymer* **2001**, *42*, 9091–9095.
- (2) Bal, M.; Ursache, A.; Goldbach, J. T.; Russell, T. P.; Tuominen, M. T. *Appl. Phys. Lett.*, in press.
- (3) Guarini, K. W.; Black, C. T.; Milkove, K. R.; Sandstrom, R. L. *J. Vac. Sci. Technol. B* **2001**, *19*, 2784–2788.
- (4) Zehner, R. W.; Sita, L. R. *Langmuir* **1999**, *15*, 6139–6141.
- (5) Yokoyama, H.; Mates, T. E.; Kramer, E. J. *Macromolecules* **2000**, *33*, 1888–1898.
- (6) Amundson, K.; Helfand, E.; Quan, X.; Smith, S. D. *Macromolecules* **1993**, *26*, 2698–2703.
- (7) Amundson, K.; Helfand, E.; Quan, X.; Hudson, S. D.; Smith, S. D. *Macromolecules* **1994**, *27*, 6559–6570.
- (8) Thurn-Albrecht, T.; DeRouchey, J.; Russell, T. P.; Jaeger, H. M. *Macromolecules* **2000**, *33*, 3250–3253.
- (9) Mansky, P.; DeRouchey, J.; Russell, T. P.; Mays, J.; Pitsikalis, M.; Morkved, T.; Jaeger, H. *Macromolecules* **1998**, *31*, 4399–4401.
- (10) Huang, E.; Pruzinsky, S.; Russell, T. P.; Mays, J.; Hawker, C. J. *Macromolecules* **1999**, *32*, 5299–5303.
- (11) Mansky, P.; Russell, T. P.; Hawker, C. J.; Mays, J.; Cook, D. C.; Satija, S. K. *Phys. Rev. Lett.* **1997**, *79*, 237–240.
- (12) Mansky, P.; Liu, Y.; Huang, E.; Russell, T. P.; Hawker, C. *Science* **1997**, *275*, 1458–1460.
- (13) Mansky, P.; Russell, T. P.; Hawker, C. J.; Pitsikalis, M.; Mays, J. *Macromolecules* **1997**, *30*, 6810–6813.
- (14) Russell, T. P.; Thurn-Albrecht, T.; Tuominen, M.; Huang, E.; Hawker, C. J. *Macromol. Symp.* **2000**, *159*, 77–88.
- (15) Mansky, P.; Harrison, C. K.; Chaikin, P. M.; Register, R. A.; Yao, N. *Appl. Phys. Lett.* **1996**, *68*, 2586–2588.
- (16) Bouas-Laurent, H.; Castellán, A.; Desvergne, J.-P.; Lapouyade, R. *Chem. Soc. Rev.* **2000**, *29*, 43–55.
- (17) Greene, F. D.; Misrock, S. L.; James, R. Wolfe, J. *J. Am. Chem. Soc.* **1955**, *77*, 3852–3855.
- (18) Bouas-Laurent, H.; Castellán, A.; Desvergne, J.-P. *Pure Appl. Chem.* **1980**, *52*, 2633–2648.
- (19) Schlenk, W.; Bergmann, E. *Justus Liebigs Ann. Chem.* **1928**, *463*, 1–322.
- (20) Martin, E. L. *J. Am. Chem. Soc.* **1936**, *58*, 1438–1442.
- (21) Laarhoven, W. H. *Tetrahedron* **1970**, *26*, 4865–4881.
- (22) Stolka, M.; Yanus, J. F.; Pearson, J. M. *Macromolecules* **1976**, *9*, 710–714.
- (23) Hruska, Z.; Vuillemin, B.; Riess, G.; Katz, A.; Winnik, M. A. *Makromol. Chem.* **1992**, *193*, 1987–1994.
- (24) Coursan, M.; Desvergne, J. P. *Macromol. Chem. Phys.* **1996**, *197*, 1599–1608.
- (25) Tong, J. D.; Zhou, C.; Ni, S.; Winnik, M. A. *Macromolecules* **2001**, *34*, 696–705.
- (26) Tong, J. D.; Ni, S.; Winnik, M. A. *Macromolecules* **2000**, *33*, 1482–1486.
- (27) Tcherkasskaya, O.; Ni, S.; Winnik, M. A. *Macromolecules* **1996**, *29*, 610–616.
- (28) Ni, S.; Zhang, P.; Wang, Y.; Winnik, M. A. *Macromolecules* **1994**, *27*, 5742–5750.
- (29) Bartz, T.; Klapper, M.; Müllen, K. *Macromol. Chem. Phys.* **1994**, *195*, 1097–1109.
- (30) Odriscoll, K.; Sanayei, R. A. *Macromolecules* **1991**, *24*, 4479–4480.